Estimating the Probability of Failure of a Dike due to Post-Liquefaction Settlements

Laura Luna[1], Dr. Gordon Fenton[1], and Dr. Roberto Olivera[2]
[1]*Department of Engineering Mathematics, Dalhousie University, Halifax, NS*
[2]*Golder Associates Ltd. Vancouver, BC, Canada*

ABSTRACT
The objective of this study is to estimate the probability of failure of a simplified dike system due to excessive post-liquefaction reconsolidation settlements of the foundation soils. The results are presented in the form of seismic fragility curves, which estimate the probability of failure of a performance level as a function of peak ground acceleration. The curves are obtained by combining 1-dimensional liquefaction triggering analyses with Monte Carlo simulations, with soil strength being modelled as a 2-dimensional spatially correlated random field. The study considers four performance levels, determined in accordance with seismic design guidelines and field performance data. Additionally, the effects of horizontal correlation length and dike system length on the estimated probabilities are explored. Site-specific seismic hazard models may then be used to obtain the total probability of dike failure over its design lifetime.

RÉSUMÉ
L'objectif de cette étude est d'estimer la probabilité de défaillance d'un système de digues simplifié en raison des tassements excessifs de reconsolidation post-liquéfaction des sols de fondation. Les résultats sont présentés sous forme de courbes de fragilité sismique, qui estiment la probabilité de défaillance d'un niveau de performance en fonction de l'accélération maximale du sol. Les courbes sont obtenues en combinant des analyses de déclenchement de liquéfaction à une dimension avec des simulations de Monte Carlo, où la résistance du sol est modélisée comme un champ aléatoire à corrélation spatiale bidimensionnelle. L'étude considère quatre niveaux de performance, déterminés conformément aux directives de conception sismique et aux données de performance sur le terrain. De plus, les effets de la longueur de corrélation horizontale et de la longueur du système de digues sur les probabilités estimées sont explorés. Des modèles d'aléa sismique propres au site peuvent ensuite être utilisés pour obtenir la probabilité totale de défaillance d'une digue pendant sa durée de vie nominale.

1 INTRODUCTION

The Lower Mainland of British Columbia has the unique challenge of being subject to a combination of high seismic and flood hazards, which leads to major challenges in the design of flood-protection infrastructure.

As the region densifies and increasingly relies on earthen dikes as a major flood-defense mechanism, there are growing concerns about the ability of these geotechnical systems to survive major earthquake events.

Many of these dikes are founded on loose saturated soils, making liquefaction of the foundation soils during an earthquake event a major concern. The objective of this study is to estimate the probability of failure of a simplified dike system due to excessive liquefaction induced settlements, and to develop seismic fragility curves specific to this failure mode.

The fragility curves (sometime called system response curves) are obtained through a combination of simplified 1-dimensional liquefaction triggering analyses and Monte Carlo simulations using random field realizations to model the spatial variability of the foundation soils in the horizontal and vertical directions. The probability of failing to meet specified performance levels is calculated for a variety of peak ground accelerations (PGAs) considering the contribution of different earthquake magnitudes. The analyses also explore the effect that horizontal correlation length and the length of the dike system have on the estimated probabilities of failure.

The fragility curves developed can be later combined with site-specific seismic hazard models that relate shaking intensity measures to the return period of the earthquake event to yield the overall probability of failing each performance level over the design lifetime of the system. The results can thus be integrated into a more generalized risk-assessment framework for flood-protection dikes, which should account for other potential failure modes as well as consider the consequences associated with failing to meet each performance target.

2 DEFINITION OF FAILURE

A critical step of any risk-based design is the definition of what conditions constitute a *failure* of the geotechnical system. In general, a *failure* condition does not necessarily imply complete collapse, as it may also refer to the failure of the system to meet an intended function. Thus, it is important to clearly define what is referred to herein as *failure*.

In the context of flood-protection dikes, *failure* will be taken as any condition which compromises the flood-protection ability of the dike. This may occur due to a complete collapse of the dike body, or in less severe cases, due to small or moderate cracks in the dike body as well as loss of the minimum required freeboard. The probability of each of these events occurring, the role of human intervention, as well as the cost associated with their consequences, must be accounted for in any risk-based approach. The task is then to decide on quantifiable levels of dike damage.

Current seismic design guidelines for high-consequence dikes in British Columbia (Atukorala et al., 2014) prescribe a performance-based design approach of flood-protection dikes, wherein different levels of earthquake ground motions are paired with acceptable levels of damage. The guidelines specify three performance categories (A, B, and C), corresponding to no significant damage, some repairable damage, and significant damage to the dike body, respectively. Performances A and B specify that the post-seismic flood protection ability must not be compromised, whereas it may be possibly compromised in Performance C. Performances A, B, and C are matched with earthquake shaking levels corresponding to 100-year, 475-year, and 2,475-year return periods, respectively. Under these seismic events, designers must ensure the predicted deformations are within a set of allowable displacements, which were established "with the intent of preserving the structural integrity of the dike" (Atukorala et al., 2014), i.e., designed against failure.

Useful case study observations on the performance of dikes following strong shaking are available in the literature. For example, Kwak et al. (2016) systematically examined the performance of dikes along the Shinano River system in Japan after two crustal earthquakes of magnitude 6.6. The study classified observations into one of five damage levels, ranging from slight damage with small cracks to full levee collapse. Each damage level had reported ranges of settlements after the earthquake.

This study considers a combination of the BC seismic design guidelines for dikes and the observed field performance data in Japan. Four performance categories are established, as shown in Table 1.

An important distinction between this probability-based approach and a performance-based one is that in this study there is no specific earthquake shaking level associated with each performance level. Instead, the probability of exceeding each one of the levels specified in Table 1 is calculated for a range of possible earthquake peak ground acceleration (PGA) levels, and may then be combined with the probability of occurrence of each event using site-specific seismic hazard models to obtain the total probability of failure of a dike over a design time period.

Table 1. Dike Performance Levels from Design Guidelines and Field Performance Data

Performance Level	Maximum Crest Settlement	Description
A	0.10 m	Slight damage, small cracks.[1]
B	0.15 m	No significant damage to dike.[2]
C	0.30 m	Moderate damage, cracks.[2]
D	0.50 m	Significant damage.[1]

[1]As prescribed in design guidelines (Atukorala et al., 2014).
[2]As described in field performance data (Kwak et al. 2016).

3 METHODOLOGY

The probability of failure of a dike system of a given length due to excessive post-liquefaction reconsolidation settlements is estimated using simplified 1-dimensional liquefaction-triggering analyses combined with Monte Carlo simulations. The simulations use spatially correlated random fields to model the normalized cone penetration resistance (q_{c1Ncs}), thus accounting for the variability of the foundation soils. A schematic of the problem set-up is shown in Figure 1.

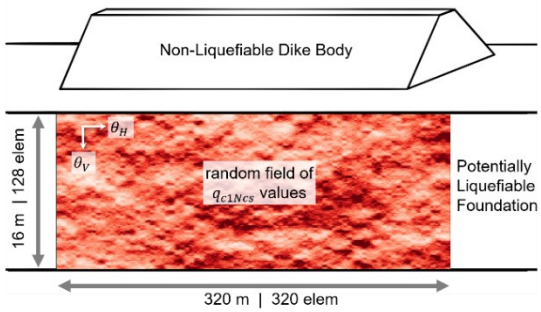

Figure 1. Schematic of problem set-up.

The steps followed to estimate the probability of failure of the above system are as follows:

1) Create a 2-D spatially correlated random field to model the spatial variability of the foundation soils.
2) For each soil column in the random field, complete a 1-dimensional simplified liquefaction triggering analysis and estimate the post-liquefaction reconsolidation settlements for a given peak ground acceleration (PGA), accounting for the probabilistic nature of earthquake magnitude (see section 5.2).
3) Determine whether the dike segment has failed each specified performance level. For the dike segment to have *failed*, five adjacent soil columns (corresponding to a 5 m stretch of the dike) must have settlements exceeding the maxima of the performance level.

   To examine the effects of dike length on the probability of failure, repeat this step while considering sub-segments of the field of increasing widths, centered at the midpoint of the dike. This

study considered seven different dike lengths (see section 6.4).

4) Repeat steps 1 to 3 for different realizations of the random field (number of simulations in this study was 5,000 for each correlation structure).
5) Calculate the probability of failure at a given PGA by counting the number of failed segments, and dividing by the total number of realizations.
6) Repeat steps 1 to 5 for values of PGA ranging from 0.05 g to 0.50g in increments of 0.01g. This step yields curves of probability of failure of a performance level against PGA for different dike lengths.
7) Repeat the above steps for different horizontal correlation lengths, to examine the effect of anisotropy on the estimated probabilities of failure (see section 6.3). This study considered nine different correlation structures.

4 RANDOM SOIL MODEL

To account for the spatial variability of the strength of dike foundation soils, cone penetration resistance (q_{c1Ncs}) was modelled as a 2-dimensional stationary random process. Random fields were generated using the Local Average Subdivision (LAS) method, as described in Fenton & Griffiths (2007). The two dimensions of the field represent depth below the soil surface and distance along the dike crest. That is, the random fields run parallel along the dike alignment.

The fields were created considering a depth of 16 m and a maximum dike length of 320 m, with resolution of 128 by 320 elements, respectively. Cone resistance was assumed to follow a lognormal distribution with a mean of 100 kPa and a coefficient of variation of 15%, as shown in Figure 2.

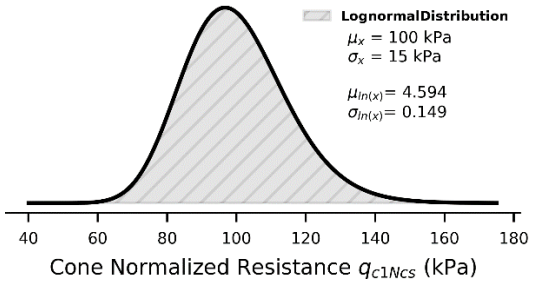

Figure 2. Assumed lognormal distribution of normalized cone penetration resistance.

Spatial correlation in the horizontal and vertical directions was modelled using an exponentially decaying Markov function of the form:

$$\rho(\tau) = exp\left(-\frac{2|\tau|}{\theta}\right) \quad [1]$$

which prescribes the correlation coefficient (ρ) between two points separated by a distance (τ) as a function of the correlation length (θ), which may be loosely defined as the distance at which two soil properties cease to be significantly correlated.

To explore the potential effects of anisotropy on the reliability of the dikes, the vertical correlation length was held constant at $\theta_v = 1\,m$, while several correlation lengths in the horizontal direction were considered ranging between 0.25 m and 500 m, as displayed in Figure 3.

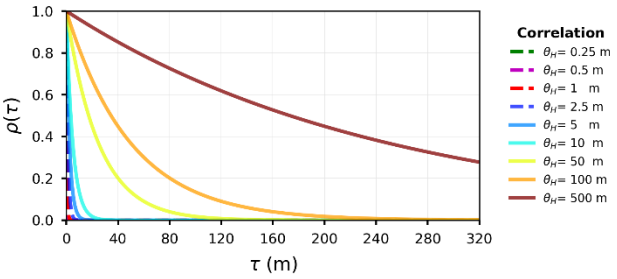

Figure 3. Markov correlation functions considered in the horizontal direction.

5 ESTIMATION OF POST-LIQUEFACTION RECONSOLIDATION SETTLEMENTS

Seismic-induced displacements in dikes can be evaluated through Nonlinear Deformation Analyses using dynamic finite element or finite difference methods. When conducting nonlinear analyses, vertical crest displacements and loss of freeboard can develop in two primary ways: (1) vertical displacements caused by shear deformation of the soil associated with lateral spreading and (2) settlement caused by reconsolidation of the liquefied soil.

Most constitutive models, however, are not able to simulate the post-liquefaction reconsolidation effects since a large portion of the volumetric strains is due to sedimentation effects, which are not easily incorporated into the modelling algorithms. This paper presents a methodology to develop fragility curves to examine the failure of dikes due to reconsolidation effects after the cessation of shaking.

Post-liquefaction reconsolidation settlements were calculated by examining each soil column within the random fields separately, and using traditional simplified 1-dimensional methods to estimate the settlements at varying PGAs and earthquake moment magnitudes.

5.1 Factor of Safety against Liquefaction

First, the factor of safety against liquefaction for each random field element was determined based on the typical triggering correlation, as a ratio of the cyclic resistance ratio (CRR) to the cyclic stress ratio (CSR):

$$FS_{liq} = \frac{CRR_{M=7.5,\ \sigma'_{vc}=1}}{CSR_{M=7.5,\ \sigma'_{vc}=1}} \quad [2]$$

The cyclic resistance ratio for each element was calculated using the following relationship, developed by Boulanger and Idriss (2016) based on a liquefaction case-history database:

$$CRR_{M=7.5,\ \sigma'_{vc}=1} = exp\left[\frac{q_{c1Ncs}}{113} + \left(\frac{q_{c1Ncs}}{1{,}000}\right)^2 - \left(\frac{q_{c1Ncs}}{140}\right)^3 + \left(\frac{q_{c1Ncs}}{137}\right)^4 - 2.60\right] \quad [3]$$

The cyclic stress ratio was calculated using the simplified relationship presented by Idriss and Boulanger (2008):

$$CSR_{M=7.5,\ \sigma'_{vc}=1} = 0.65 \cdot PGA \cdot r_d \cdot \frac{\sigma_{vc}}{\sigma'_{vc}} \frac{1}{MSF} \frac{1}{K_\sigma} \quad [4]$$

where σ_{vc} and σ'_{vc} are the total and effective vertical stresses, respectively, MSF is the magnitude scaling factor, r_d is the shear stress reduction coefficient, and K_σ is the overburden correction factor. These factors were calculated deterministically in accordance with Idriss and Boulanger (2008) using updated relationships for the magnitude scaling factor (MSF) presented in Boulanger and Idriss (2015).

A deterministic bulk unit weight of 20kN/m^3 was used to estimate the vertical stresses, and all elements were assumed to be fully saturated (i.e., it was assumed that the water table is at the ground surface).

5.2 Post-Liquefaction Vertical Strains

The estimated vertical strains were computed using the simplified method initially proposed by Ishihara and Yoshimine (1992), as presented in Idriss and Boulanger (2008), which prescribes the reconsolidation strains as a function of normalized cone penetration resistance as well as the maximum shear strains developed during undrained cyclic loading, as follows:

$$\varepsilon_v = 1.5\ exp(2.551 - 1.147(q_{c1Ncs})^{0.264})\ min(0.08,\ \gamma_{max}) \quad [5]$$

The method ignores the topographic and the shear bias effects caused by the dike slopes on liquefaction development and lateral spreading. The maximum shear strains are also estimated from simplified relationships proposed by Yoshimine et al. 2006 as presented in Idriss and Boulanger (2008). The maximum shear strain is a function of the estimated factor of safety against liquefaction, and may be calculated as follows:

$$\gamma_{max} = \begin{cases} 0\ if\ FS_{liq} \geq 2 \\ min\left(\gamma_{lim}, 0.035(2 - FS_{liq})\left(\frac{1-F_\alpha}{FS_{liq}-F_\alpha}\right)\right)\ if\ F_\alpha < FS_{liq} < 2 \\ \gamma_{lim}\ if\ FS_{liq} \leq F_\alpha \end{cases} \quad [6]$$

where the limiting strain and alpha function are calculated as:

$$\gamma_{lim} = 1.859\ (2.163 - 0.478(q_{c1Ncs})^{0.264})^3 \geq 0 \quad [7]$$

$$F_\alpha = -11.74 + 8.34(q_{c1Ncs})^{0.264} - 1.371(q_{c1Ncs})^{0.528} \quad [8]$$

The settlements are then calculated by integrating the vertical strains over the depth profile.

5.3 Probabilistic Treatment of Earthquake Magnitude

The process described in sections 5.1 and 5.2 was repeated for increasing values of peak ground acceleration, ranging from 0.05 g to 0.50 g. As it is current practice to complete liquefaction triggering analyses using a site-specific probabilistic PGA as prescribed in Canada's seismic hazard model, the magnitude deaggregation method as described in Finn et al. (2016) was used to account for the contribution of different earthquake magnitudes to the overall seismic hazard.

The magnitude deaggregation method uses the magnitude-distance deaggragation of the seismic model to obtain magnitude bins with associated relative contribution to the hazard (%). Then, a calculation analogous to the total probability theorem may be used to determine the predicted settlements for a given PGA.

This approach was used for the current study, using the same magnitude-distance deaggragation presented by Finn et al. (2016) for a site in Vancouver, as shown in Figure 4. The post-liquefaction reconsolidation settlements were determined for each earthquake moment magnitude shown in Figure 4 (ranging from 5.1 to 8.9) and for each PGA. The results were then multiplied by the appropriate relative contribution to the hazard and added together to yield the final estimated settlements for a given PGA value.

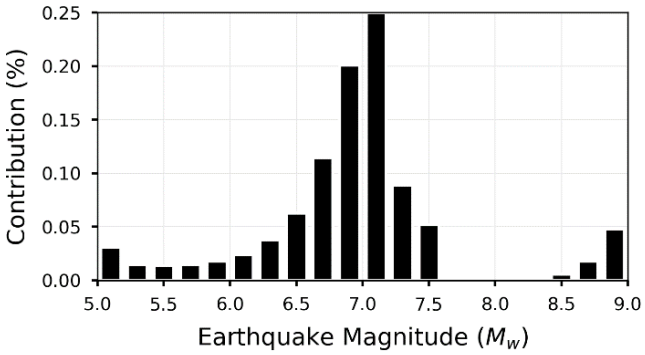

Figure 4. Relative contribution of earthquake magnitudes to the seismic hazard for a site in Vancouver

6 PROBABILITY OF FAILURE: SEISMIC FRAGILITY CURVES

6.1 Results for the *Median Soil Column*

It is helpful to first determine the predicted post-liquefaction settlements without introducing spatial variability, in order to provide a baseline to which the probabilistic results can be compared.

Using the methods described in Section 5, the settlements as a function of PGA were calculated for a soil column with normalized cone penetration resistance values all equal to the mean of the probability distribution presented in Figure 2. From this curve, shown in Figure 5, the PGA at which each performance level is *failed* can be easily obtained based on the maximum settlement criteria outlined in Table 1 (scatter points in Figure 5).

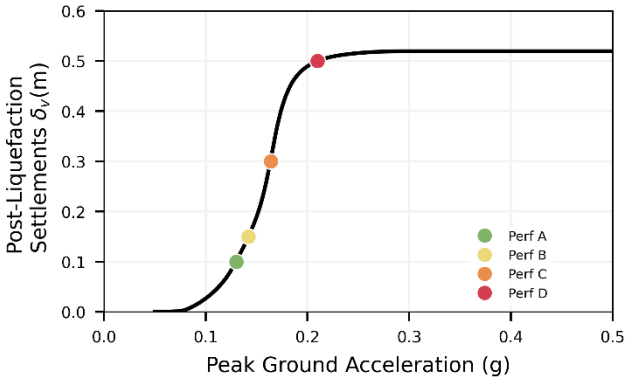

Figure 5. Post-liquefaction reconsolidation settlements vs. PGA for a soil column with median strength.

It is important to note that the above curve is specific to a liquefiable depth of 16 m. Since the median q_{c1Ncs} value is 98.89 kPa, and since equation 5 has a cap on the maximum shear strain at 8%, then the maximum vertical strain that may be predicted is 3.2%. This strain is reached once PGA values reach roughly 0.23 g or greater. Thus, the maximum settlement is capped at 0.52 m.

Since this scenario does not consider spatial variability, the probability of failure vs. PGA curve results in a piece-wise function that goes vertically from a probability of 0 to a probability of 1 at a critical PGA value, as shown in Figure 6, below.

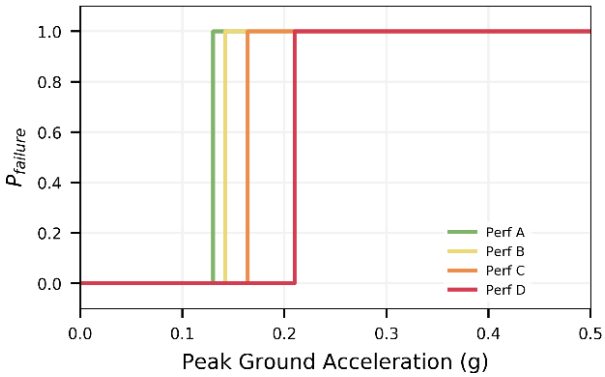

Figure 6. Probability of failure of each performance level for the median soil column.

6.2 Incorporating Spatial Variability

Using the methodology outlined in section 3, spatial variability is incorporated to estimate the probability of failure vs. PGA curves for a dike of length 301 m. These curves may be referred to as seismic fragility curves, as they indicate the probability of reaching or exceeding a damage state under a specific earthquake excitation. The resulting curves are shown in Figure 7. Each curve displayed corresponds to different assumed values of horizontal correlation length.

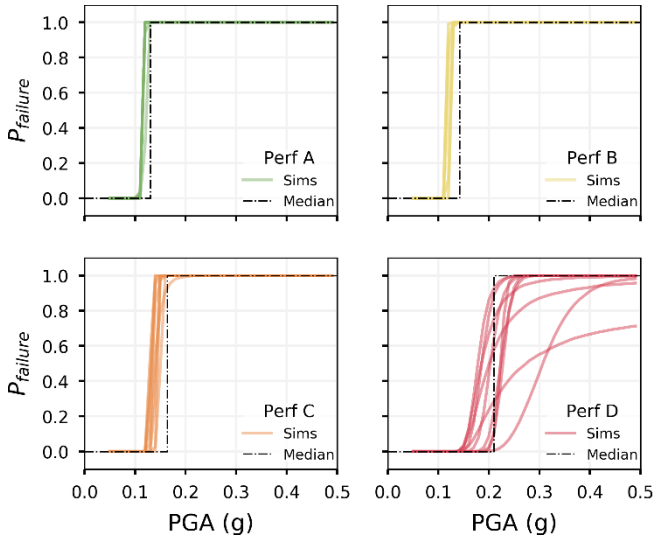

Figure 7. Seismic fragility for a 301 m long dike for various horizontal correlations and 4 performance levels.

The above results indicate that the first three performance levels (A, B, and C) are somewhat insensitive to the assumed horizontal correlation length. In general, the results from these three performance levels follow the piece-wise function obtained from the median soil column reasonably closely. These results are similar across the different dike lengths considered (11m to 301m).

It is unsurprising that the probabilities of failure exceed zero at smaller PGA values than the critical PGA of the median soil columns. Allowing for randomness in soil strength values inevitably results in some soil columns with low strength values. As the reconsolidation settlement calculation is highly sensitive to normalized cone penetration resistance, this variability has a measurable effect on the probabilities of failure

The increase in the allowable settlement for performance level D results in more dependence in correlation length and more deviation from the median soil column. This dependency is further complicated when considering different dike lengths.

The following sections explore the effects of horizontal correlation length and dike length on the estimated seismic fragility functions for all the performance levels.

6.3 Effects of Horizontal Correlation Length

As discussed in the previous section, the effects of horizontal correlation length on the estimated seismic fragility functions is most notable for performance level D. Nonetheless, the effect is still observed for performance levels A, B, and C. Figure 8 displays the seismic fragility functions for a dike length of 301 m for varying values of horizontal correlation length for performance levels A, B, and C.

Since the choice of horizontal correlation length is most influential for performance level D, a comparison is presented in Figure 9 for three different dike lengths (11 m, 101 m, and 301 m). As before, the seismic fragility curves are compared to the results from the median soil column.

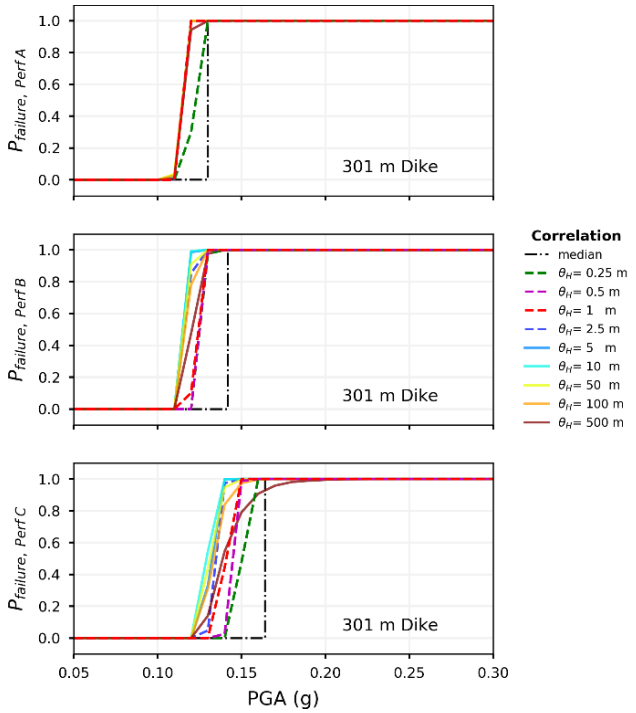

Figure 8. Seismic fragility functions with varying horizontal correlation for performance levels A, B, and C.

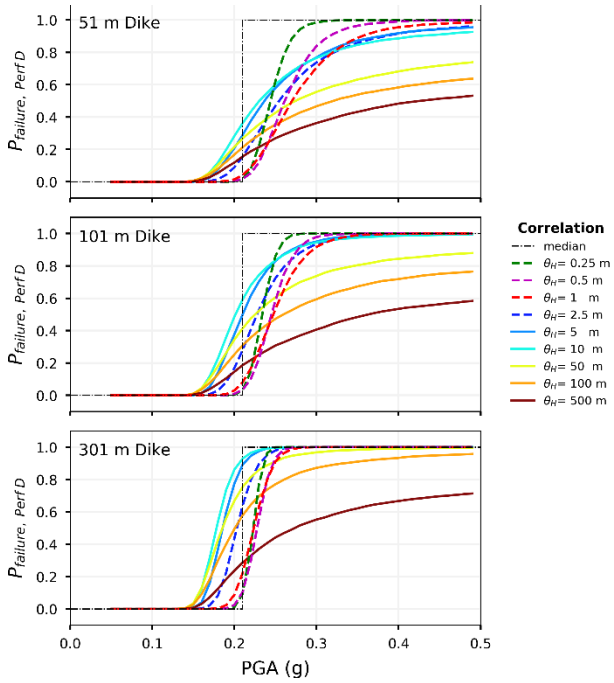

Figure 9. Seismic fragility functions with varying horizontal correlation and dike length, for performance level D.

The results in Figures 8 and 9 show that the effects of horizontal correlation length depend on the value of the assumed correlation length θ. Two different effects are at play:

$For\ \theta_H \leq 5$: As the horizontal correlation length approaches and then becomes smaller than the width of the random field elements, the values of all individual elements will have a tendency to average towards the median value of the q_{c1Ncs} distribution shown in Figure 2 (towards the median and not the mean, because the field is lognormally distributed). As a result, reductions in horizontal correlation length yield curves that approach the median curve.

$For\ \theta_H \geq 5$: As the correlation length increases and eventually approaches the total length of the random field, there is a tendency towards more uniform fields. That is, each random field realization is less variable, with most elements having similar values. However, each realization of the field draws randomly from the original distribution. Since each random field is more uniform, it is overall less likely that a given realization will fail. This then results in seismic fragility curves with generally lower probabilities of failure for increasing correlation lengths.

6.4 Effects of Dike Length

Without carrying out complex analyses, it is straightforward to infer how the length of a dike affects the overall geotechnical system reliability: when all other aspects are held equal, longer dikes should have higher probabilities of failure than shorter dikes. This is simply because there are more locations for potential *weak spots* where failure may occur in longer dikes.

This effect, commonly referred to as the *length effect*, has been extensively studied in the context of slope stability analyses or piping failure modes (see for example Li & Hicks, 2014; Lopez de la Cruz et al., 2011; and Vanmarcke, 2011). Different approaches have been proposed to address the issue.

A simplified approach described by Wolff (2008) consists of dividing a dike system into geologically similar reaches. If the length of the reach is less than the correlation length, then the probability of failure of a 2D cross-section is taken as the probability of failure of the reach. Otherwise, if the length of the reach is greater than the correlation length, then the reach it is divided into segments with length equal to the correlation length.

A more comprehensive and elegant approach was presented by Vanmarcke (2011), which treats the limit state function as a random process dependent on the location along the dike, and uses “threshold-crossing analysis” to determine the overall probability that the system will survive.

Since a simulation approach was taken in this study, the effects of dike length on the overall probability of failure can be quantified by examining incrementally larger dike segments, as described in section 3.

The results of this procedure are displayed in Figure 10 for performance levels A, B, and C, considering a horizontal correlation length of 50 m. Sample results for

performance level D are shown in Figure 11 for horizontal correlation lengths of 5 m, 50 m, and 500 m.

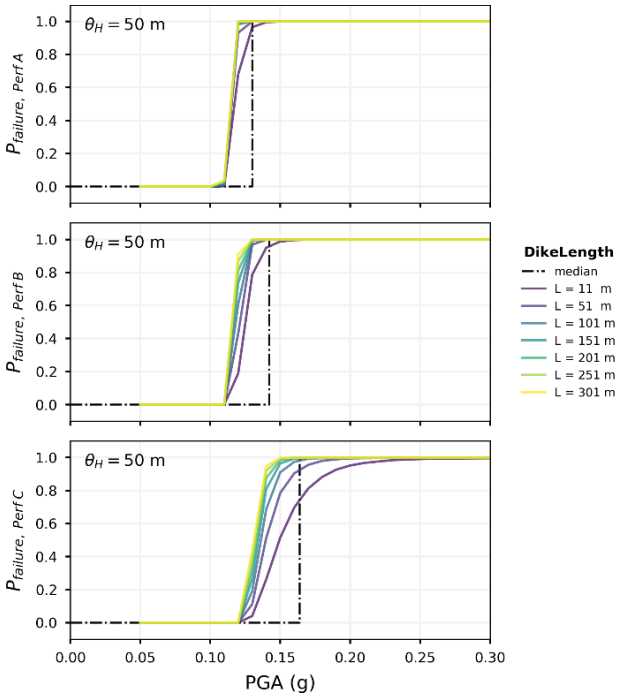

Figure 10. Seismic fragility functions for dike segments of varying length, for performance levels A, B and C.

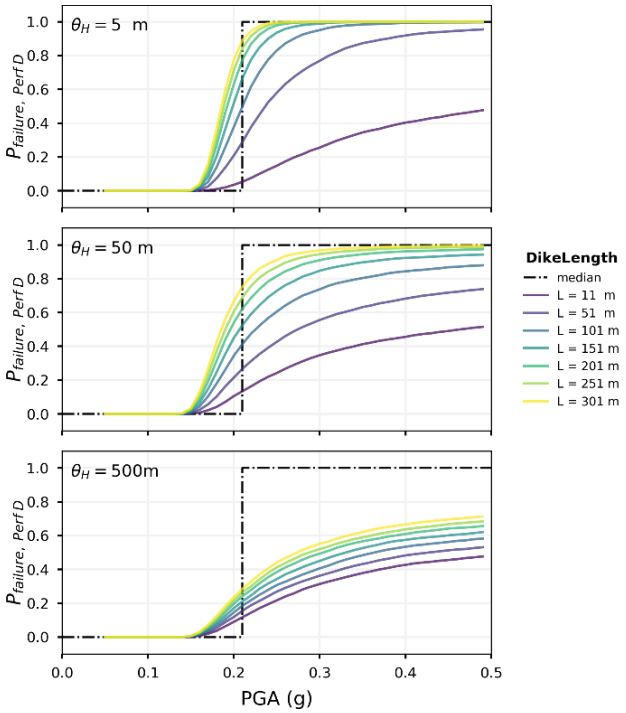

Figure 11. Seismic fragility functions for dike segments of varying length and horizontal correlation lengths, for performance levels D.

As was the case when examining correlation length effects, the effects of dike length on the seismic fragility curves is least influential for the probability of failing performance level A (smallest allowable settlements), and most influential for the probability of failing performance level D (largest allowable settlements).

In Figures 10 and 11, it is evident that shorter dike segments lead to lower probabilities of failure. Figure 11 also shows that the difference in probabilities becomes more pronounced for smaller values of horizontal correlation length. These results hold true for all the correlation lengths considered, but not all are displayed for the sake of brevity. Additionally, the effects of dike length are also more significant for larger values of peak ground acceleration.

Another approach to visualize the dike length effect is to plot the probability of failure for given PGA values as a function of dike length. An example of this approach is shown in Figure 12.

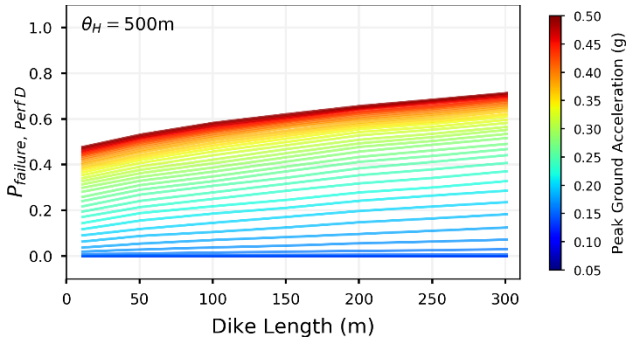

Figure 12. Probability of failing performance level D as a function of dike length, for several values of PGA.

7 CONCLUSION

Through the combination of simplified 1-dimensional liquefaction triggering analyses and Monte Carlo simulations, this study has developed seismic fragility curves for a simplified dike system. The fragility curves present the probability of failing a given performance level as a function of peak ground acceleration and are specific to the failure mode of excessive post-liquefaction reconsolidation settlements of the underlying foundation soils.

The spatial variability of the foundation is accounted for by modelling normalized penetration resistance as a 2-dimensional random field with distinct vertical and horizontal correlations structures. The two dimensions represent depth below the ground surface and distance along the dike alignment.

The effects of horizontal correlation length on the estimated probabilities of failure are described, and are found to manifest in two separate ways: as the correlation length becomes smaller than the random field elements, the fragility curves approach the curve corresponding to the media soil column.

However, as the correlation length approaches the total domain size, the random fields become more uniform and the probabilities of failure decrease for increasing correlation lengths.

As expected, increases in the length of the dike system result in an increase in probability of failure for all performance levels and correlation structures considered.

To obtain the overall probability of failure of the dike over the design lifetime, the seismic fragility curves may be combined with site-specific seismic hazard models that prescribe the return period associated with each shaking level. The results of this study may then be integrated into a generalized risk-assessment for dikes that considers other potential failure modes and quantifies the consequences of failing to meet each performance criteria.

The proposed methodology sheds light on the effects of the correlation distances in the foundation soils on the evaluation of post-liquefaction settlements. The next step in this study would be incorporating the probability of failure considering vertical displacements caused by shear deformation of the soil associated with lateral spreading. The overall probability of failure presented in the paper is therefore expected to increase once these effects are incorporated into the fragility curves previously presented. The study could also be repeated for different distributions of shear strength parameters, to examine how the results are affected by the shear strength of the foundation soils.

8 ACKNOWLEDGEMENTS

The authors are thankful for the support provided by the Natural Sciences and Engineering Research Council of Canada.

9 REFERENCES

Atukorala, U., Hawson, H., Mylleville, B., & Williams, R. (2014). Seismic design guidelines for dikes (2nd ed.). Ministry of Forests, Lands and Natural Resource Operations, Flood Safety Section.

Boulanger, R. W., & Idriss, I. M. (2016). CPT-Based Liquefaction Triggering Procedure. Journal of Geotechnical and Geoenvironmental Engineering, 142(2), 04015065.

Boulanger, R. W., & Idriss, I. M. (2015). Magnitude scaling factors in liquefaction triggering procedures. Soil Dynamics and Earthquake Engineering, 79, 296–303.

Fenton, G., & Griffiths, D. (2007). Random field generation and the local average subdivision method. In Probabilistic methods in geotechnical engineering (Vol. 491, pp. 201–223).

Finn, W. D. L., Dowling, J., & Ventura, C. E. (2016). Evaluating liquefaction potential and lateral spreading in a probabilistic ground motion environment. Soil Dynamics and Earthquake Engineering, 91, 202–208.

Idriss, I. M., & Boulanger, R. W. (2008). Soil liquefaction during earthquakes. Earthquake Engineering Research Institute.

Ishihara, K., & Yoshimine, M. (1992). Evaluation of settlements in sand deposits following liquefaction during earthquakes. Soils and Foundations, 32(1), 173–188.

Kwak, D. Y., Stewart, J. P., Brandenberg, S. J., & Mikami, A. (2016). Characterization of Seismic Levee Fragility Using Field Performance Data. Earthquake Spectra, 32(1), 193–215.

Lopez de la Cruz, J., Calle, E. O. F., & Schweckendiek, T. (2011). Calibration of Piping Assessment Models in the Netherlands.

Vanmarcke, E. (2011). Risk of Limit-Equilibrium Failure of Long Earth Slopes: How It Depends on Length. GeoRisk 2011, 1–24.

Wolff, T. (2008). Reliability of levee systems. Reliability-Based Design in Geotechnical Engineering, 448–496.